Werk

Jahr: 1980
Kollektion: fid.geo
Signatur: 8 Z NAT 2148:47
Digitalisiert: Niedersächsische Staats- und Universitätsbibliothek Göttingen
Werk Id: PPN1015067948_0047
PURL: http://resolver.sub.uni-goettingen.de/purl?PPN1015067948_0047

LOG Id: LOG_0043
LOG Titel: Reykjanes Ridge crest studied by surface waves with an earthquake-pair technique
LOG Typ: article

Übergeordnetes Werk

Werk Id: PPN1015067948
PURL: http://resolver.sub.uni-goettingen.de/purl?PPN1015067948
OPAC: http://opac.sub.uni-goettingen.de/DB=1/PPN?PPN=1015067948

Contact

Niedersächsische Staats- und Universitätsbibliothek Göttingen
Georg-August-Universität Göttingen
Platz der Göttinger Sieben 1
37073 Göttingen
Germany
Email: gdz@sub.uni-goettingen.de

J. Geophys. 47, 265–270, 1980

Journal of Geophysics

Reykjanes Ridge Crest Studied by Surface Waves With an Earthquake-Pair Technique

C.E. Keen[1], A. Fricker[1], M.J. Keen[1], and L. Blinn[2]

[1] Atlantic Geoscience Centre, Geological Survey of Canada, Bedford Institute of Oceanography, Dartmouth, Nova Scotia, Canada
[2] Department of Oceanography, Dalhousie University, Halifax, Nova Scotia, Canada

Abstract. Dispersion of surface waves generated by earthquakes beneath the Reykjanes Ridge is used to find a model for the shear-wave velocity as a function of depth beneath a young crestal region. The Reykjanes Ridge and the WWSSN observatory AKU in Iceland lie close to a great circle, so it is possible to separate dispersion generated by paths on the Ridge itself from the total dispersion, which includes the effects of Iceland, using an adaptation of the station-to-station technique. As there are no pairs of stations, pairs of earthquakes are used; cross-correlation and filtering of the surface wave trains yields the travel times between earthquakes – and so the group velocities – at different periods. The observed dispersion of Love waves and Rayleigh waves seen over two paths along the Ridge are modelled using Backus-Gilbert inversion techniques, varying shear-wave velocities with depth. The periods used are 6 to 18 s (Love) and 6 to 37 s (Rayleigh). Velocities in the crust (to 6.45 km) are fixed from seismic refraction observations. Model velocities below this increase to 4.3 km/s at 20 km, reflecting a high-velocity lid, and decrease to 4.0 km/s by 40–50 km, reflecting the low-velocity zone. The base of this zone is not seen because the periods used are not sufficiently long, but it must lie below 100 km. This model can be interpreted in terms of a zone of partial melting only a few tens of kilometres wide below the high-velocity lid; a density model based upon this feature can account for the observed gravity field.

Key words: Reykjanes Ridge crest – Surface wave dispersion upper-mantle structure – Gravity.

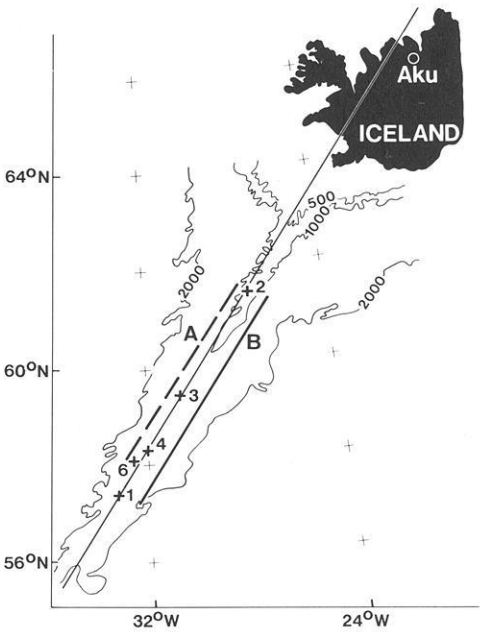

Fig. 1. The Reykjanes Ridge and Iceland. Bathymetric contours are in metres. Path *A* lies between events 2 in the north and 4 and 6 in the south; path *B* lies between events 2 and 1. The *long solid line* shows the great-circle path along the Ridge

Introduction

Studies of the crust and mantle of crestal regions of mid-ocean ridges are important because new lithosphere forms beneath such regions, and an understanding of the processes of lithosphere formation requires a knowledge of the physical properties underneath the ridge crests. Some experiments, such as long-range refraction experiments, are difficult or expensive to do; observations of heat-flow near crestal regions may be difficult to obtain, or hard to interpret (Sclater et al., 1976). Deductions from dispersion of surface waves may be ambiguous because of the geometrical relationships between sources and receivers, the paths crossing oceanic provinces belonging to a great range of ages; consequently a path which is restricted to a region of uniform age with uniform properties along the path, would be valuable (Forsyth, 1975). Earthquakes along the Reykjanes Ridge, recorded at the WWSSN station AKU in northern Iceland provide such a path beneath the crestal region of a mid-ocean ridge (Fig. 1). In this report we describe how surface waves travelling along this path lead us to shear-wave velocities within young crust and mantle.

We need to determine group velocity as a function of period for Rayleigh or Love waves or both, but one of the two methods most commonly used renders results difficult to interpret, the other cannot be applied. If there is a single source and a single station present interpretation techniques require that the earth between is laterally homogeneous. This would clearly be an improper assumption to make because most of Iceland lies between the Reykjanes Ridge and AKU. Paths of more restricted length – and so, hopefully, with more laterally uniform properties beneath – can often be obtained by using two stations with a single source beyond the line joining the two stations. Dispersion caused by the earth between the source and the closer station is, in essence, 'subtracted' from the dispersion observed at the farther station, leaving only the dispersion caused by the earth between the stations (Landisman et al., 1969). However, there is only one station along the path Reykjanes Ridge–Iceland, and so instead of using pairs

0340-062X/80/0047/0265/$01.20

of stations we restrict the path lengths over which we measure dispersion to the Rekjanes Ridge itself by choosing pairs of earthquakes. The Ridge and AKU bear a convenient geometrical relationship one to another, so that pairs can be chosen which lie on a great circle from AKU. The effect of the earthquake closer to AKU is 'subtracted' from the effect of the earthquake farther from AKU to leave the dispersion due only to the earth beneath the path between the earthquakes. In principle, this should yield results identical to the more usual 'pure-path' techniques, but in this case we obtain group velocities between sources, instead of stations.

Figure 1 shows the locations of earthquake sources used in this study, in relation to the position of AKU. Each source location is the site of more than one event, usually a main shock followed by a sequence of aftershocks, so that a number of dispersion curves can be obtained for the same path. This allows mean dispersion curves to be calculated and errors to be estimated. The data have been divided between two paths, A and B, where the events at location 2 are common to both (Fig. 1). This division into two paths was made because (a) the paths are somewhat different, and (b) it yields some assessment of the effects of different source mechanisms. Since shear velocities have been estimated independently along each path this allows some estimate of the validity of the method to be made.

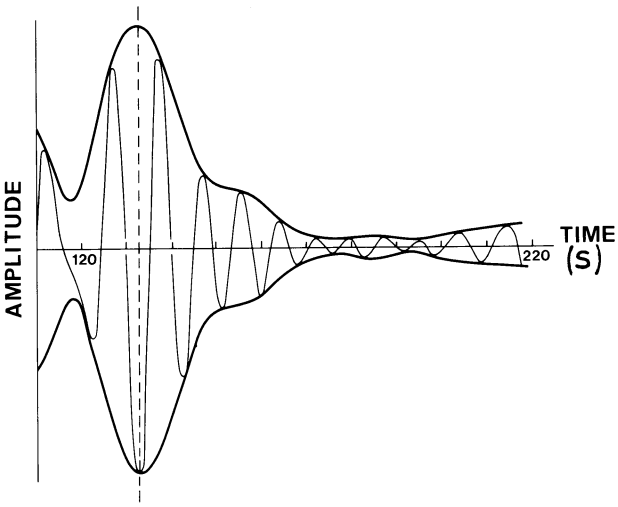

Fig. 2. The filtered cross-correlogram for the pair 2A–4D, vertical component. Central filter period 9.9 s, event-to-event distance 436.6 km. The peak in the envelope at 132 s gives the group arrival time of signal energy at the central filter period

Analysis of Data

Our concern is to determine group velocities of surface waves generated by an earthquake as a function of period for a segment of a ridge crest. We can then compare these (experimental) velocities with the (theoretical) values generated from a model, and so obtain estimates of the model parameters which control the model group velocities – in this case, shear-wave velocity as a function of depth. Consequently we need to find the travel time of phases over a range of periods between two points on the ridge crest, knowing the distance between them.

Briefly, we obtain the Fourier transform of a pair of seismograms, $f_1(t)$, $f_2(t)$, generated by a source at either end of Path A or B (Fig. 1) and received at AKU. Cross-multiplication in the frequency domain, the equivalent of cross-correlation in the time domain, gives the phase difference as a function of frequency between the seismograms and removes the effect of the propagation paths lying between the station and the event closest to it. The cross-correlated spectrum is filtered using the Gaussian filter

$$G(\omega) = A\, e^{-a(\omega-\omega_0)^2}$$

centred at frequency ω_0 for which we seek the group velocity. The advantage of this filter is that it gives the optimum resolution of both time (or group velocity) and frequency (Robinson, 1967). Here the parameter, a, was chosen to give equal fractional uncertainty in both group velocity and period (Fricker, 1971). Inverse Fourier transformation of the filtered signal allows the arrival time of the energy centred on ω_0 to be obtained. Figure 2 shows an example of a typical filtered and inverse-transformed cross-correlogram. The envelope's peak defines the group arrival time centred on ω_0.

Nine earthquakes from the four locations, 1, 2, 4, and 6, were chosen from all occurring on the Reykjanes Ridge between March, 1962 and March, 1972 with body wave magnitudes $m_b > 4.7$ (Table 1). Their reported depths are the reference depth of 33 km, not the actual depths, likely to be in the range of 5 (or less) to 10 km (Weidner and Aki, 1973).

The records of all components were photo-enlarged three times, and digitized with a D-MAC pencil follower at intervals of approximately 1.5 s (and all maxima and minima); cubic spline iterpolation was used to give evenly spaced data points at 0.75 s. The digitized seismograms were windowed, and the spectra found using a fast Fourier Transform algorithm; these spectra were corrected for the instrument response at AKU. The Rayleigh and Love modes were resolved using the horizontal and vertical components. In the case of Love waves the horizontal motion normal to the wave path (assumed to be the great circle path) was found from the east-west and north-south spectra; in the case of Rayleigh waves we usually used only the vertical spectra, because of higher noise levels associated with the horizontal spectra (so that the enhancement of signal to noise anticipated using horizontal components along the wave path together with the vertical component could not be realized).

The events were set in pairs, so that each event from one site could be cross-correlated with all events at a second site. This led to ten dispersion curves along path A, and four along path B, corresponding to events 2 and 4, 2 and 6 (Path A) and 2 and 1 (Path B) (Tables 1 and 2). The spectral records, resolved for Rayleigh and Love modes, were then cross-multiplied and filtered as described already. Group velocities were found for periods of 6 to 37 s for fundamental Rayleigh mode and 6 to 18 s for fundamental Love mode, the limits being selected on the basis of digitizing interval, signal energy, and the wavelengths at long periods – which become comparable to path length.

Because there are a number of pairs of earthquakes for each path, we can calculate mean values and standard errors of the group velocities at each period. The methods used are described only briefly here; details are given in Fricker (1971, 1976). The errors leading to differences in values of velocity are of two sorts. Errors common to all periods in one dispersion curve lead to general differences in 'level' between curves of velocity versus period for the different earthquake pairs, and are due to: mislocation of earthquakes; error in origin time; fault zones of finite length; and long-term drift in instrument response not seen in calibration. These errors can be partly removed by 'sliding' together the velocity-period curves using as criteria for adjustment

Table 1. Earthquake sources

No.	Date	Time	Lat. °N	Long. °W	m_b	Azimuth°	Dist km
1A 1972	June 19	06:00:51.1±0.99	57.37±0.033	33.43±0.036	5.0	228.3	1,227.9
1B 1972	June 19	12:14:27.0±0.96	57.39±0.029	33.38±0.031	4.8	228.2	1,224.3
2A 1966	May 05	15:25:12.5≡0.21	61.49±0.040	27.40±0.048	4.7	228.8	655.9
2B 1966	May 05	15:52:40.9±0.15	61.45±0.031	27.49±0.040	4.9	228.9	662.4
4A 1969	September 20	00:56:52 ±1.3	58.27±0.054	32.15±0.054	4.9	228.1	1,102.1
4B 1969	September 20	01:07:41 ±1.1	58.29±0.043	32.03±0.046	5.0	227.8	1,096.2
4C 1969	September 20	01:03:07 ±1.2	58.19±0.044	32.05±0.046	5.1	227.6	1,106.0
4D 1969	September 20	05:08:57.8±12	58.35±0.029	32.08±0.030	5.6	228.2	1,092.5
6A 1968	September 14	01:38:42.6±0.28	58.08±0.061	32.64±0.060	5.1	228.6	1,136.1

Notes: These data have been taken from the Bulletin of the International Seismological Centre, Edinburgh, Scotland. Distances to AKU were calculated using a spheroidal earth. Azimuths are the great-circle directions from the station towards the event

Table 2. Earthquake pairs for paths A and B

Pair	Path length (km)	Azimuth°
	Path A	
2A–4A (1)	446.2	228.5
2A–4B (2)	440.3	228.3
2A–4C (3)	450.1	228.2
2A–4D (4)	436.6	228.5
2B–4A (6)	439.7	228.5
2B–4B (7)	433.8	228.4
2B–4C (8)	443.6	228.2
2B–4D (9)	430.1	228.5
2A–6A (5)	480.2	228.7
2B–6A (10)	473.7	228.8
	Path B	
2A–1A (1)	572.0	228.6
2A–1B (2)	568.5	228.5
2B–1A (3)	565.5	228.6
2B–1B (4)	561.9	228.6

Note: Numbers in brackets are those shown in Figs. 3 and 4

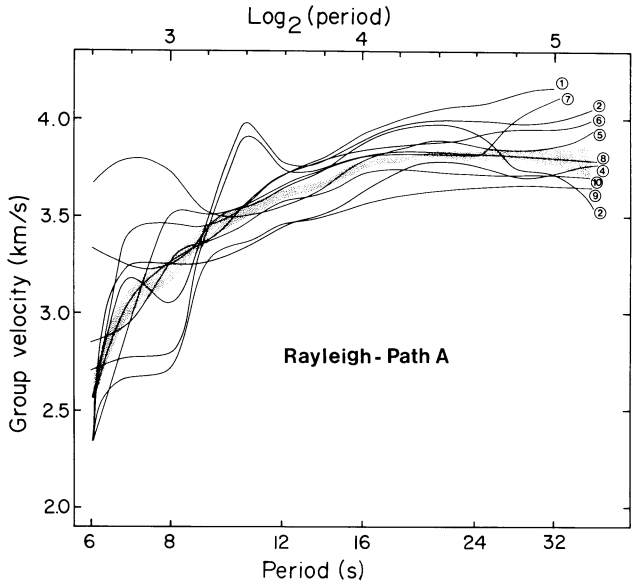

Fig. 3. Group velocity versus period for *Path A, Rayleigh.* The *solid curves* show the observations for different pairs. *Each number* designates a particular pair, given in Table 2.The shading encompasses one standard error on each side of the mean curve (see text). Observations made at increments of 0.2 on the log scale

the condition that the mean overall remains unchanged, and by seeing that the standard errors are minimized (in the least-squares sense). The errors which remain are random and due to: digitization; source mechanism; and noise. In addition, 'structural' effects between sources – sloping interfaces, for example – and interference by higher mode Love waves may make interpretation difficult. The second type of errors are random errors and lead to 'wiggles' in the curves, not necessarily coherent from one curve to another. It is from these that the standard errors used here have been calculated.

The mean group velocity at any period is calculated after the errors common to all periods from each curve, as described above, are removed in the following way (Fricker, 1976). The arrival time at a particular period will be in error because of contamination by noise and the effects of the filter used to isolate the period. Consequently weights are assigned to each value on a group velocity versus period curve which are functions of filter parameter, period, and the signal to noise ratio. These weights give value to each point on a curve inversely proportional to the likely error in travel-time, which can be calculated (in terms of the factors mentioned). Means and standard errors are calculated from the weighted values of travel time (in essence, reciprocals of group velocity). The standard errors themselves should not fluctuate markedly from period to period, and are smoothed using a binomial smoothing scheme. These smoothed standard errors, due only to random errors, are used when modelling. The curves of mean group velocity versus period should themselves vary smoothly from period to period, and so are smoothed (and interpolated) by cubic spline smoothing. The periods at which group velocities were determined are shown on Figs. 3 and 4.

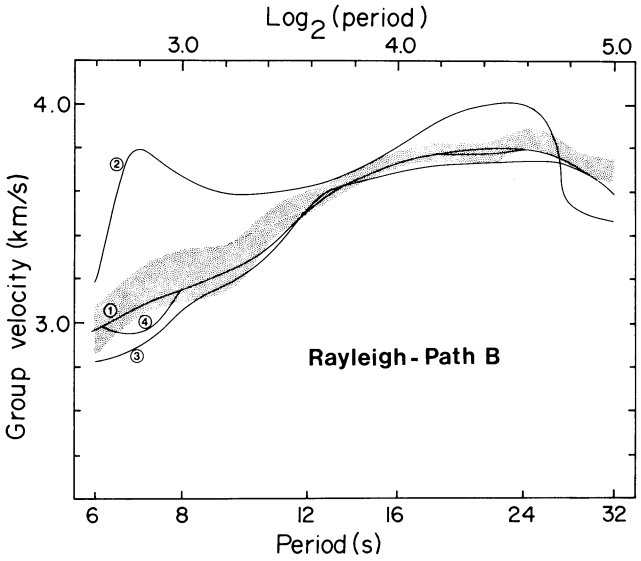

Fig. 4. Group velocity versus period for *Path B, Rayleigh.* The *solid curves* show the observations for different pairs. *Each number* designates a particular pair, given in Table 2.The shading encompasses one standard error on each side of the mean curve (see text). Observations made at increments of 0.2 on the log scale

Figures 3 and 4 show the Rayleigh wave group velocity curves before any corrections for errors and smoothing have been applied as well as the band of values falling within one standard error unit of the mean, calculated as described above. Note that the fluctuation in the individual group velocity curves has been strongly reduced in the final curves and that the standard errors are appreciably less than those which might be estimated from the scatter of the individual curves. The differences between the standard errors shown and those which might seem intuitively reasonable, which are about five times greater, are due partly to the weighting of the individual curves. However, the standard errors shown are probably underestimates. The justification for the use of these smaller errors is that the linearized inversion scheme applied to the data to obtain a shear-velocity model becomes unstable if larger errors are used, and hence the use of the smaller error estimates represents a compromise between obtaining a model by means of the inversion technique and the need to rely on modelling techniques which give no estimates of the precision and resolution of the final models. The latter would be necessary if larger errors were used.

The weakest link in the method of analysis applied here is that the behaviour of all the source functions is assumed to be the same and hence no corrections have been made for the effect of the source function and the phase as a function of frequency. While all the earthquakes are located on the Reykjanes Ridge crest, away from known fracture zones, and hence may have similar focal mechanisms representative of normal faulting, the effects of small differences in fault plane orientation and dip on the data has not been established, mainly because most of the earthquakes were not large enough to obtain reliable fault plane solutions. In addition, variations in velocity perpendicular to the ridge crest causing lateral refraction of the propagating waves have not been considered here. These effects, while important, would not in our opinion, change the basic results of the study but they should be considered in any further studies of this type.

Modelling

Models of shear velocity as a function of depth were obtained from the dispersion data, using linear inversion techniques (Backus and Gilbert, 1970). The use of these methods for surface wave studies has been described by Wiggins (1972) and specific details of the computations used in this study are given by Fricker (1976). The linear inversion method gives us both models which fit the data to within specified error limits and also estimates of the uncertainties of the models.

Theoretical data are calculated using Haskell's (1953) matrix formulation which approximates the elastic properties of the real earth by a stack of horizontal layers, each with uniform compressional and shear-wave velocities and density. The values of these parameters are varied iteratively until all the theoretical data calculated from a particular model agree with the observations to within predetermined error limits, usually one standard deviation. For rapid digital computation, the Haskell matrices have been modified as described by Schwab and Knopoff (1970), among others.

If we start with an initial model which is close to the desired model, the required changes in the parameters necessary to bring the theoretical data, calculated from the model, into agreement with the observations may be estimated by the size of the partial derivatives of the theoretical data parameters with respect to the model parameters.

The derivatives with respect to shear-wave velocities are much larger than those of compressional wave velocity or density. Variations of V_p and ρ affect the final model by an order of magnitude less than V_s. Thus V_p and ρ were not varied in producing the final models but were held at fixed values corresponding to the initial model. This starting model, as stated above, must be sufficiently close to the final result that the partial derivatives are valid indicators of the adjustments needed in the model to fit the data. Thus a certain amount of trial and error modelling is required before proceeding to the final inversion. In this study, we found that the calculated group velocities are very sensitive to water depth and the thickness of the first crustal layer. This problem was overcome by constraining the shear-wave velocities of the upper crustal layers to be in reasonable accord with the compressional wave data for the Reykjanes Ridge described by Talwani et al. (1971), and by setting the water depth at 1.62 km – a reasonable mean value for paths used. Trygvasson (1962) has shown that the effects of sloping water interfaces on Rayleigh wave dispersion curves are small at periods greater than 8 s; Love waves are of course not affected at all. In addition, the group velocities at the periods considered here have no bearing on the model below 150 km. Therefore the shear velocity was held constant at 4.33 km/s below this depth. The parameters which have been fixed during inversion are shown in Table 3; we see here that shear velocity was allowed to vary during inversion in eleven layers between depths of 6.45 km and 150 km.

Wiggins (1972) showed that for real data a limited number of model parameters can be determined if a certain degree of precision of these parameters is desired. As in other linear inverse problems a compromise must be reached between a detailed model which is poorly defined, with large uncertainties in some of the parameters, and a model which includes less detail but which is accurate to a predetermined acceptable level. This is the trade-off between resolution and precision.

The surface wave inversion method involves the solution of a set of equations using least squares minimization of the difference between theoretical and observed data (Wiggins, 1972). Thus a desired level of accuracy, the standard error of the problem, σ,

Table 3. Fixed parameters used in inversion

Depth to top of layer km	Density gm/cm^3	V_p km/s	V_s km/s
0.00	1.03	1.50	0.0000
1.62	2.84	4.20	2.1554
2.32	2.84	5.81	2.6096
3.31	2.84	6.53	3.0994
4.88	3.00	6.53	3.6752
6.45	3.20	7.20	
8.40	3.30	8.00	
9.55	3.30	8.00	
15.00	3.30	8.00	Inversion
25.00	3.30	8.00	
35.00	3.30	8.00	Parameters
40.00	3.30	8.00	
60.00	3.20	7.20	
80.00	3.20	7.20	
100.00	3.20	7.20	
125.00	3.20	7.20	
150.00	3.30	8.00	4.3300

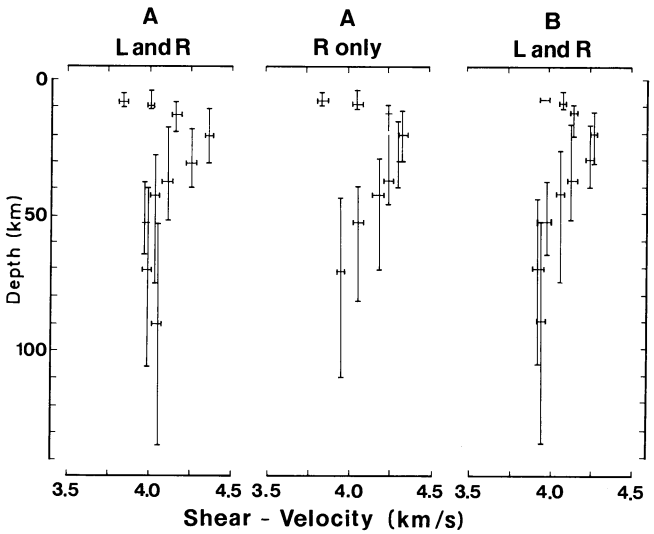

Fig. 5. Shear-velocity against depth for *Path A Love and Rayleigh (left), Rayleigh only (middle),* and *Path B Love and Rayleigh (right). Horizontal bars* give standard errors in velocity, vertical bars give the spread in depth

can be set. In this case a relative standard error of 0.01 was chosen which allows us to determine only three or four independent model parameters. This may be compared to the five parameters obtained by Forsyth (1975) for surface wave data in the Pacific. We attempted to fit both Love and Rayleigh wave data combined and Rayleigh wave data alone. Similar models were obtained in both cases, with the model data falling within about one standard error of the observations. In the case of Path A, it was not possible to obtain a really satisfactory fit to the combined Rayleigh and Love wave data, possibly because the fundamental Love mode was contaminated with higher mode interference. However, the model obtained, shown in Fig. 5, is in agreement with the other models.

The shear-velocity models are presented in Fig. 5. The horizontal bars represent the standard errors in the shear-wave velocities and the vertical bars, the depth resolution of these determinations. The resolution kernels (Backus and Gilbert, 1970) were generally compact, having a high value in only one layer. However, some degree of non-compactness was observed for the deeper layers.

A visual comparison of the shear velocity curve for Paths A and B (Fig. 5) shows no significant differences between them. At shallow depths, the shear velocity increases with depth reaching 4.3 km/s at 20 km. The velocity then decreases to about 4.0 km/s between 40 and 50 km. Below this, the resolution is not sufficient to define the base of this low-velocity zone.

Discussion

Our models showing shear-wave velocity as a function of depth are similar to those of others who have concerned themselves with young lithosphere and asthenosphere. Forsyth (1977) for example, points out that in the age range 0–5 Ma the high-velocity lid will have a velocity of 4.3 km/s, and a thickness of 30 km (or less); we see the same velocity, and his depth to the base of the lid is compatible with the marked decrease in velocity below 30–40 km demanded by our models. The velocity below this, 4.0 km/s, also agrees with Forsyth's (1977) conclusions. These similarities are significant, because the two paths we have used lie wholly along the crest of a ridge, uncontaminated by dispersion caused by other structural elements, inevitable if dispersion is measured using an earthquake-station pair, (because of the locations of the stations). This would not necessarily be true of a study such as the very interesting one of Jacoby and Girardin (1980).

The model of a low-velocity zone below 30–40 km is also in agreement with the conclusions of Solomon and Julian (1974), who, in a study of focal mechanisms of earthquakes on ridges (including one from the Reykjanes Ridge), suggested that a zone of anomalously low compressional wave velocity lay beneath the crests. They attributed this to the existence of a region of partial melting.

We have no information on the lateral extent of the low-velocity zone from our surface wave study; we can, however, model its equivalent roughly in terms of density variations, using gravity data, and compare the gravity field which would result with the observations of Talwani et al. (1971). This is done in Fig. 6; we have not tried to model lateral changes in density in the lithosphere and asthenosphere (which would be predicted by the lateral changes in shear-wave velocity suggested by Forsyth, 1977), nor are the density contrasts shown obtained from the shear-velocity models presented here, but were arbitrarily chosen. We show in Fig. 7 how our suggestion of a relatively narrow asthenospheric wedge beneath the ridge crest compares with other models.

The apparent lack of agreement near the crestal zone is hardly surprising. Parker and Oldenburg's (1973) model assumed heat to be transported by conduction, with no additional cooling by hydrothermal circulation; in their surface wave study Leeds et al. (1974) assumed that the shear-wave velocity in the high-velocity lid was 4.6 km/s (rather than 4.3 km/s near the crests) so that they could model the change in thickness of the lid with age.

It is gratifying that the technique using earthquake-pairs is in such good agreement with the studied of Forsyth (1977), and Solomon and Julian (1974). The method could perhaps be extended with profit to seek variations in velocity-depth models

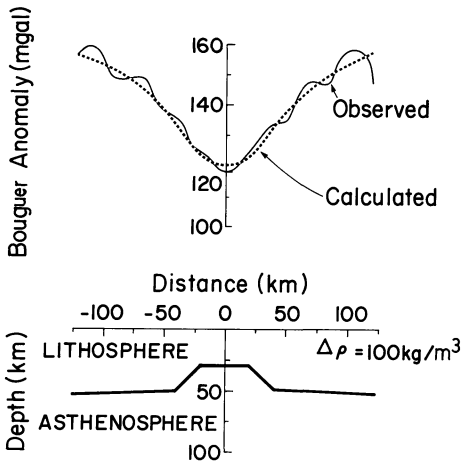

Fig. 6. The observed Bouguer anomaly across the Reykjanes Ridge (from Talwani et al. (1971) and the anomaly corresponding to the model beneath

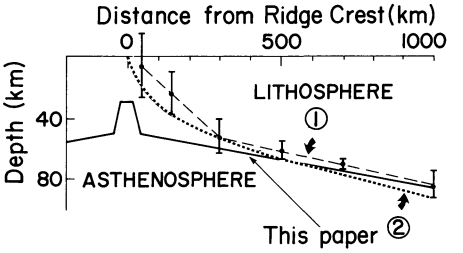

Fig. 7. Some models of the Reykjanes Ridge. The model corresponding to the density model of Fig. 6 is shown solid. *Model 1* is that derived from the surface wave study by Leeds et al. (1974) (who fixed the shear-wave velocities; see text) the vertical bars are their error limits; *Model 2* is Parker and Oldenburg's (1973) (who assumed heat transfer by conduction only; see text)

along ridge crests, seeking regional variations along particular ridges, and variations with rates of spreading. We should perhaps point out that although sophistication in modelling has been achieved using Backus-Gilbert inversion techniques, nevertheless, as they are usually applied in studies with surface waves, no account is taken of anisotropy, or lateral inhomogeneities – which in crestal regions must be significant.

Acknowledgements. We thank the National Research Council of Canada for support, and Christopher Garrett and Lynn Smith for aid. Louis Blinn and Aubrey Fricker received scholarships from Dalhousie University. Comments on the paper from D. Forsyth, R. Falconer, C. Beaumont, and S. Srivastava were most helpful.

References

Backus, G.E., Gilbert, J.F.: Uniqueness in the inversion of inaccurate gross earth data. Philos. Trans. R. Soc. London, Ser. A: **266**, 123–192, 1970

Forsyth, D.W.: The early structural evolution and anisotropy of the oceanic upper mantle. Geophys. J.R. Astron. Soc. **43**, 103–162, 1975

Forsyth, D.W . The evolution of the upper mantle beneath mid-ocean ridges. Tectonophysics **38**, 89–118, 1977

Fricker, A. A development of surface wave analysis and interpretation in the Canadian Shield. Unpublished M.Sc. Thesis, Dalhousie University, 1971

Fricker, A. Crustal models from seismic surface waves. Unpublished Ph.D. Thesis, Dalhousie University, 1976

Haskell, N.A.: Dispersion of surface waves in multilayered media. Bull. Seismol. Soc. Am. **43**, 17–29, 1953

Jacoby, W.R., Girardin, N. The evolution of the lithosphere at the southeast flank of Reykjanes Ridge from surface wave data. J. Geophys. **47**, 271–277, 1980

Landisman, M., Dziewonski, A., Sato, Y : Recent improvements in the analysis of seismic surface wave observations. Geophys. J. Astron. Soc. **17**, 369–403, 1969

Leeds, A., Knopoff, L., Kausel, E. Variations of upper-mantle structure under the Pacific Ocean. Science **186**, 141–143, 1974

Parker, R., Oldenburg, D.: Thermal model of ocean ridges. Nature Phys. Sci. **242**, 137–139, 1973

Robinson, E.A.· Statistical communication and detection. London: Griffin, 357 pp, 1967

Schwab, F.L., Knopoff, L. Surface wave dispersion computations, Bull. Seismol. Soc. Am. **60**, 321–344, 1970

Sclater, J.G., Crowe, J., Anderson, R.N. On the reliability of oceanic heat-flow averages. J. Geophys. Res. **81**, 2997–3007, 1976

Solomon, S.C., Julian, B.: Seismic constraints on ocean ridge mantle structure: anomalous fault plane solutions from first motions. Geophys. J. R. Astron. Soc. **38**, 265–285, 1974

Talwani, M.C., Windisch, C.C., Langseth, M.G.· Reykjanes Ridge crest· a detailed geophysical study. J. Geophys. Res. **76**, 473–517, 1971

Trygvasson, E. Crustal structure of the Iceland region from dispersion of surface waves. Bull. Seismol. Soc. Am. **52**, 359–388, 1962

Weidner, D., Aki, K.: Focal depth and mechanism of mid-oceanic ridge earthquakes. J. Geophys. Res. **78**, 1818–1831, 1973

Wiggins, R.A. The general linear inverse problem: implication of surface waves and free oscillations for earth structure. Rev. Geophys. **10**, 251–285, 1972

Received April 5, 1979; Revised Version August 31, 1979